Hindawi
Applied and Environmental Soil Science
Volume 2023, Article ID 6099543, 14 pages
https://doi.org/10.1155/2023/6099543

Research Article

Modeling Soil Loss and Its Association to Site Physical Characteristics in Majang Watershed, Baro Abobo River Basin

Mengie Belayneh, Mamush Masha, and Bedilu Befikadu

Department of Geography and Environmental Studies, Mattu University, Mettu, Ethiopia

Correspondence should be addressed to Mengie Belayneh; mengie1980@yahoo.com

Received 24 April 2023; Revised 5 July 2023; Accepted 8 August 2023; Published 24 August 2023

Academic Editor: Fedor Lisetskii

One of Ethiopia's threatening environmental problems is soil erosion. Minimizing soil erosion to the tolerable level needs evidence-based sustainable land management. This study aimed to investigate the soil erosion rate and its relation with site physical characteristics (slope, land use/cover, and soil properties) using the GIS-based RUSLE model in the Majang watershed. Climate data, DEM, Landsat image, and soil map were used to model soil erosion by applying the RUSLE model. The results showed that cultivated land is the most vulnerable type of land use to soil loss (35.1·t ha^{-1} $year^{-1}$) followed by grasslands (19.6·t ha^{-1} $year^{-1}$) in the watershed. Conversely, forest land is the least vulnerable land use and generates a very low amount of soil loss (12·t ha^{-1} $year^{-1}$). Similarly, the average soil loss of the watershed is strongly related to the slope gradient. The model result indicated that a high amount of soil loss was observed in very steep slope land (62.8·t ha^{-1} $year^{-1}$) but lower in the gentle slope (13.6·t ha^{-1} $year^{-1}$). Soil types and their characteristics have greater roles in generating a high amount of soil loss. Acrisols, which lack organic matter content, have experienced a high soil loss rate (20·t ha^{-1} $year^{-1}$). This implies soil loss is highly associated with site-specific characteristics such as slope gradient, land cover/use, and soil condition. The greatest share of the soil loss was estimated from steep slopes, bare and cultivated land, and less fertile soils. Therefore, building an integrated participatory approach needs immediate attention, and all farmers and stakeholders need to focus on on-site prioritization and invest more in conserving vulnerable areas.

1. Introduction

Soil erosion is an important contributor to the world's socioeconomic and environmental problems [1]. Soil erosion severity strongly varies as to the type and interaction of different site characteristics such as climate, soil characteristics, terrain features, land cover and uses, and related land management [2–4]. The problem of soil erosion has been ubiquitous in almost all agroecologies [5–8], which affected 56% of the soil globally [9]. Soil erosion accounted for about 70–90% of soil degradation at the world level [10]. For instance, gully erosion alone damaged 2.13% of the watershed area to the irreversible stage [11]. It resulted in an agricultural productivity decline of 23% in the global terrestrial area, and it either directly or indirectly affected ~3.2 billion people worldwide [12].

Soil erosion processes originated from natural and human causes [13, 14], and the complex interaction of economic, social, and environmental factors [15]. Water-induced soil erosion is a process that occurs following raindrops, saturation, and infiltration of excess surface runoff [16]. However, anthropogenic processes make it to worsen exponentially over time [17, 18]. Gürtekin and Gökçe [16] in their study presented that, besides, the natural factors that accelerate soil erosion have been caused by rapid population growth and the related administrative problems (such as creating alternative means of livelihoods opportunities and harmonizing human-environment interaction) and land management activities, which consequently resulted in environmental and negative economic effects. Although it was a problem for a long period [19], a well-known soil degradation process results mainly from anthropogenic activities and animal overpopulation. Landscape modification

by human alteration, particularly from forestland to other land uses, has had a significant impact on soil degradation, fragmentation, and habitat losses and strongly affects biodiversity [20]. Humans are changing and modifying the natural environment via their day-to-day entraction [18, 21].

Soil erosion is the most challenging environmental problem causing a significant impact on land productivity and food security in Ethiopia's highlands [22, 23]. The severe soil erosion in Ethiopia is related to human modification of the environment such as cultivation of marginal lands, overgrazing, and land cover degradation [2, 23–25].

Soil erosion results in the reductions in productivity of arable lands [26], reduced forest and woody vegetation cover [24], soil nutrient losses [2, 27], limited vegetation growth, reduction of crop production [28], a threat to the national economy [29], and sustainability of agricultural production [30]. The Ethiopian Highland Reclamation Study (EHRS) estimated a gross average soil loss of 35 t ha-^{1} year^{-1} from the highlands of Ethiopia annually [26], and two-thirds of the population has been affected by erosion [24]. Some watershed-based studies in the Ethiopian highlands focusing on sheet and rill erosion reported as high as 93·t ha^{-1} yr^{-1} average rate of erosion [31]. Cropland is most vulnerable in this case and contributes 80% of the soil loss in the highlands of Ethiopia [32].

For the last four decades, the government of Ethiopia and its development partners have been working to adopt and use different soil and water technologies to reverse soil erosion problems and improve rural livelihoods [33]. However, the majority of the techniques have not been supported with scientifically evaluated evidence, and the intervention is not mostly in priority areas [22, 34]. As a result, most of them are not successful as planned [14], and soil erosion remains the main agricultural and environmental challenge in the area [14, 33, 35, 36]. Quantitative analysis of soil erosion and area prioritization that were studied so far concentrated more in northern and central Ethiopia [2, 22, 25, 36, 37].

The southwestern part of Ethiopia (in which the current study area is part) experiencing the highest amount of rainfall annually (>2000 mm on average) received little research attention concerning the identification of erosion risk-prone areas and their relation with site-specific characteristics. The Majang watershed in the Ilu Aba Bore zone is a typical agricultural watershed in a high rainfall and rugged topography area. The area experienced a rapid expansion of cultivation at the expense of natural forest. However, the rate of soil loss and its association with site characteristics have not been well studied and documented in the southwestern high-rainfall Ethiopian highlands. Insufficient data could lead to worthless management of soil and water conservation initiatives. Therefore, the main purpose of the study was to estimate the rate of soil erosion and its association with site-specific physical characteristics using the GIS-based RUSLE model in the humid Majang Watershed, southwestern Ethiopia.

2. Materials and Methods

2.1. The Study Area. This study was conducted in Majang Watershed Bure Woreda, which is located in the Bure district of the Illubabor zone**,** Oromia regional state of Ethiopia (Figure 1). Geographically, this district is located from 8°14′45″ N to 8°16′48′ of latitude and 34°59′14″ to 35°1′57″E of longitude, with an average elevation of 1705 m above sea level. The total area of the watershed is 2169.2 hectares. The watershed is located at a distance of 694 km southwest of Addis Ababa on the main road away from the capital city of Ethiopia to Gambella and 98 km from Mettu town.

The watershed has two typical agroecological zones, of which 47.4% is Woina Dega and 52.6% is Kola. The maximum and minimum temperature of the area is 24.1 and 15.5 C, respectively. The temperature range is between 14.2 and 23 C in the wet season and 24 and 27°C in the dry season. The mean annual rainfall ranges between 1013 and 1959 mm. The highest rainfall is recorded in June and August and the lowest is from December to February. The watershed experiences two rainy seasons that is the Belg and Kiremt. The Belg is a short rainy season occurred in March, April, and May. The Kiremt season is known to be the longest rainy season, covering June, July, August, and September. The rainfall that occurs during the Kiremt season is very intensive, and the severity of soil erosion is high during these months (*Bure District Agriculture and rural development office* [38]). Kiremt is the season in which most of the crop is cultivated.

2.2. Data Types, Sources, and Method of Acquisition. The necessary input data for this study were the digital elevation model, rainfall data, land use/land cover maps, and soil data (Table 1). In this regard, 22 years of the rainfall data record of four stations (Bure, Masha, Gore, and Gambella) were interpolated by 30 m grid cells using the inverse distance weighted interpolation method. The inverse distance weighted interpolation method was applied and recommended to generate an erosivity map for the watershed surface area [39]. The erosivity factor (R) for the study was calculated using the collected rainfall data. Cloud-free Landsat 8 OLI (Operational Land Images) satellite image with 30 m resolution was downloaded from the United Nations Geological Survey (USGS) website at path 169, row 55 on February 27/2021. The digital soil map covering the study area was taken from the digital soil map of the Baro Abobo Basin. The Baro Abobo Basin Authority has developed a soil map of the basin in a vector data format with a 1 : 250,000 scale. Besides, the DEM of the study area was downloaded from http/www.usgs.gov.com, and the topo sheet (0835C4, 1986) and study area shape file were taken from the Ethiopian Geospatial information agency. The LS factor was derived from the DEM collected from the USGS website. Reference data and land use land cover classification validation coordinate points were collected from the field using handheld GPS.

2.3. Method of Soil Loss Estimation. The Universal Soil Loss Equation developed by Wischmeier and Smith [40] is the most frequently used empirical soil erosion model worldwide. Renard et al. [41] have modified the USLE into a Revised Universal Soil Loss Equation (RUSLE) by

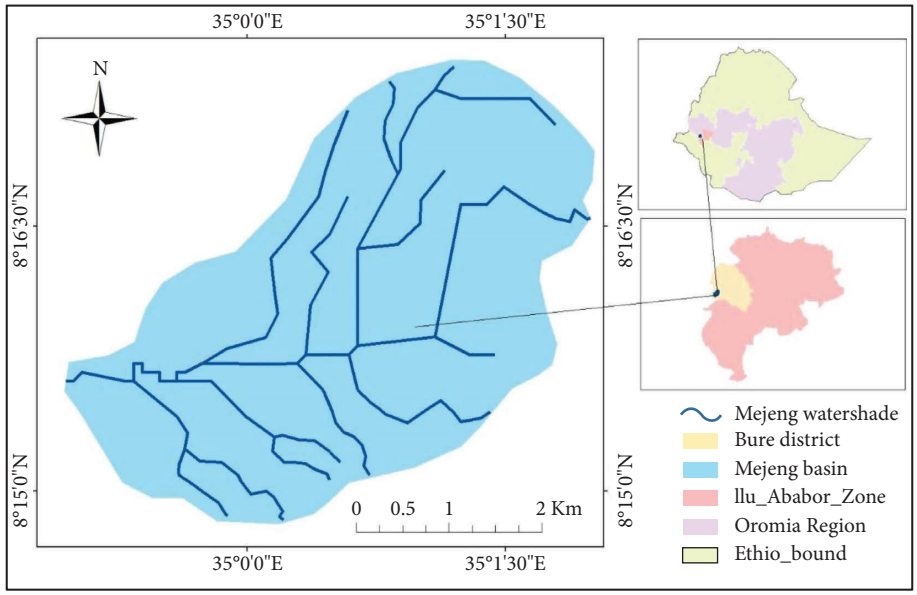

Figure 1: Map of the Majang watershed.

Table 1: Data types, sources, and quality used in the RUSLE model.

Data	Sources	Quality
Climate data	National metrological station of Ethiopia	22 years of monthly data
Soil data	Digital soil map of the Baro Abobo basin	1 : 250,000
Landsat imageries	http/www.usgs.gov.com	30 m
Topo sheet map	Ethiopian geospatial information agency	1 : 50,000
DEM	http/www.usgs.gov.com	30 m
GCP	Field survey using hand-held GPS	±3 m

introducing improved means of computing the soil erosion factors. Besides, Hurni [42] modified some factors of the RUSLE for Ethiopian conditions. Hurni (39) made at least three modifications such as computing the erosivity of rainfall, cover factor computation, and land use management factor. The model estimates the loss of soil by considering rainfall data, soil property, topographic factors, cover management, and conservation practices (equation (1)).

$$A = R * K * \mathrm{LS} * C * P, \quad (1)$$

where A is the average annual soil loss (t ha^{-1} year-^{1}), R is the rainfall and runoff erosivity factor (MJ mm ha^{-1} h^{-1} year^{-1}), K is a soil erodibility factor (t ha^{-1} MJ^{-1} mm^{-1}), LS is a slope length and slope steepness factor, C is the land cover or crop management factor, and P is a support practice or erosion control practice factor. The model was simulated under a GIS environment as shown in Figure 2.

2.3.1. Rainfall Erosivity Factor (R-Factor). The erosivity of rainfall is the quantitative expression of its potential to cause erosion in a given circumstance and represents the erosive force of specific rainfall [43]. The erosivity factor (R) was calculated according to the equation given by [42], derived from spatial regression analysis [44] for Ethiopian conditions. It was modified in the real situations of Ethiopia by [42] based on the available mean annual rainfall data. Thus, this study used Hurni's [42] empirical equation (equation (2)).

$$R = -8.12 + (0.562 \times P), \quad (2)$$

where R is the R-factor value (MJ mm ha^{-1} h^{-1} yr^{-1}) and P is the mean annual rainfall in mm

Twenty-two years of monthly rainfall data from four surrounding stations were taken from Ethiopian National Meteorology Agency (Table 2). It was then interpolated by inverse distance weighted method with 30 m grid cells. The average annual rainfall data were computed for 22 years to find the long-term mean annual rainfall of the area.

2.3.2. Erodibility of the Soil (K-Factor). The soil data used for the Majang watershed were obtained from the digital soil map of the Baro Abobo basin in a vector format. The soil map of the watershed was extracted from the Baro Abobo basin soil map and three types of soil (Dystric Nitisols, Orthic Acrisols, and Dystric Cambisols) have been identified. The K-value for each soil type was assigned depending on the type of soil and its color as suggested by Hurni [42]. The soil map in vector format was converted into a 30 × 30 m raster map using its K-value in ArcGIS® 10.3 conversion tools.

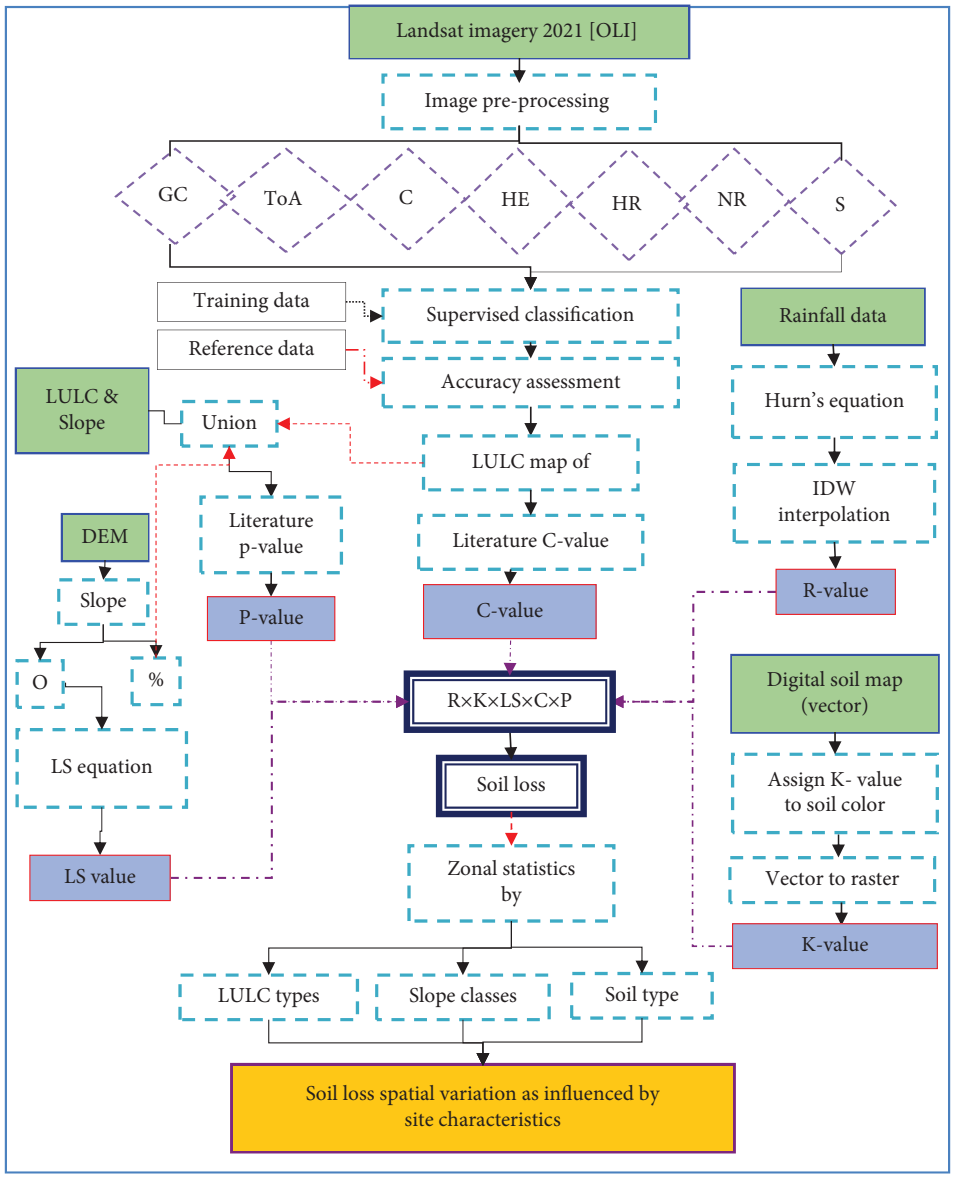

Figure 2: Flowchart of soil loss estimation and mapping using the RUSLE model. Note: GE is a geometric correction, ToA is top of atmospheric reflectance, C is c-correction, HE is histogram equalization, HR is haze reduction, NR is noise reduction, and S is layer stacking.

Table 2: Rainfall stations, locational information, their mean annual rainfall, and *R*-value of selected rainfall stations.

No.	Stations	Latitude (*Y*)	Longitude (*X*)	Mean annual rainfall (mm)	*R*-factor
1	Masha	7°30′42.80″N	35°24′52.11″E	1968	1182.55
2	Bure	8°19′29.71″N	35°2′14.46″E	1687	1029.52
3	Gore	8°8′30.09″N	35°32′42.02″E	1822	1156.17
4	Gambella	8°15′42.73″N	34°37′28.23″E	1228	976.072

2.3.3. Slope (LS-Factor). The topographic effect of soil erosion modeling in the RUSLE equation has been shown in the slope length (*L*) and the slope steepness factors [45]. It can increase the erosivity of runoff through the increased velocity of runoff water [2]. As a result, the water travels at a higher speed on steeper slopes and consequently increases its shear stress on the surface and transportation of greater sediment [40]. The slope length (*L*) is the ratio of soil loss from field slope length to that of 22.13 m length under specific conditions [40]. The LS factor is the ratio of soil loss per unit area from a field slope to that from a 22.13 m length of uniform 9% slope under otherwise identical conditions [40]. For the LS estimation, a pixel size of 30 m ASTER global digital elevation model (GDEM) was used. The DEM was

geometrically corrected and extracted by the extent of the watershed. Following the DEM preprocessing, the slope analysis such as flow direction, flow accumulation, and filling sinks was performed. Lastly, the value of "L" was specified by using the following equation [41]:

$$L = \left(\frac{X_h}{22.13}\right)^m, \tag{3}$$

where X_h is the horizontal slope length *(m)* and m is the exponent of the variable slope as it is defined to the ratio ε of rill erosion to inter-rill erosion which is calculated as $m = \varepsilon/1 + \varepsilon$, successively ε is computed for the soil erosion, which is moderately susceptible to rill and inter-rill erosion and simplified as the following:

$$\mathbf{m} = \left(\frac{\boldsymbol{\beta}}{(\mathbf{1} + \boldsymbol{\beta})}\right), \boldsymbol{\beta} = \left(\frac{\mathbf{sin}\,\theta/\mathbf{0.0896}}{\left[\mathbf{3.0}\,(\mathbf{sin}\,\theta)^{\mathbf{0.8}} + \mathbf{0.56}\right]}\right), \tag{4}$$

where θ is the slope angle.

Moreover, the ratio of soil loss from field slope to 9% slope under the specific conditions, the S factor of RUSLE equation is calculated as the following [41]:

$$\begin{aligned} S &= 10.8 \times \sin\theta + 0.03, \quad \sigma \leq 9\%, \\ S &= 16.8 \times \sin\theta - 0.50, \quad \sigma > 9\%, \end{aligned} \tag{5}$$

where S is the slope steepness factor, θ is the slope angle, and σ is the slope gradient in percentage.

The steepness and length determine the capacity of the runoff to sediment transport [46]. Moreover, LS does not consider the complexity of the topography but simply assumes soil loss increases with slope length [47]. Hence, it is better to consider the three-dimensional topography and the upslope important area to better understand the spatial distribution of soil erosion and the process of deposition. In this regard, the authors of [48] developed a calculation to compute the length-slope factor in ArcGIS from the DEM using the following equation:

$$\mathrm{LS} = \left(\frac{\mathrm{As}}{22.13}\right) \times \left(\frac{\sin\theta}{0.0896}\right), \tag{6}$$

where LS is the topographic factor, as is the upslope contributing area divided by the width of the contour that area contributes, θ is the slope angle in degree ($m = 0.4$–0.6 and $n = 1.2$-1.3), and the exponent value m has given the value of 0.4 while the value of n is equal to 1.3 [46, 49].

2.3.4. Cover Factor (C-Factor). The C-factor is used within the RUSLE to reflect the effect of cropping and management practices on erosion rates, compare the relative impacts of management options on conservation plans, and measure the combined effect of all the interrelated cover and management variables [40]. Therefore, to determine the *C*-value, the land use/cover classification map approach was selected for this study as it gives a comparatively precise *C*-value than the normalized difference vegetation index (NDVI). Therefore, satellite imageries were collected to classify the land use land cover of the watershed.

(1) Land Use/Cover Classification. The dry season captured image has been selected to develop a land use/cover map of the area. The dry season was selected to minimize crop and grass effects during the land use land cover classification. As a result, February was considered to be the optimum month for the land use land cover analysis. Before the classification of the image, different image enhancement preprocessing has been performed as image preprocessing such as layer stacking, geometric correction, haze reduction, DN conversion, and subsetting. This was employed to make the map suitable and easy for the intended classification. In this regard, a 1 : 50,000 topo sheet map was employed for the geometric rectification of the satellite image. The atmospheric and radiometric corrections were conducted to reduce the noise effects of the images. The area of interest (AOI) that covers the Majang watershed was subsetted using ERDAS IMAGINE 2014. The classification of geometrically corrected Landsat images begins with defining the training area. The training points were collected from the field using a hand-held GPS.

Land use types were identified based on the researchers' knowledge of the area and the reconnaissance survey conducted during the year 2021. Accordingly, land use/cover classes of the area were identified as cultivated land, shrub land, grazing land, forest patches, and settlement. The image was then classified following a supervised classification in the maximum likelihood algorithm technique, and the analysis was performed using ERDAS 2014 software.

The ground truth data collected from the field were used as a reference for image classification. The total sampled ground truth data collected from the field were (256 reference data) stratified consistently to each LULC class. The reference data were used to examine the classification accuracy of the LULC images. In this regard, the error matrix and kappa coefficient were used to evaluate the accuracy of the produced image and the consistency of the reference data. Overall, the classified image has an accuracy of 87% and a Kappa coefficient of 0.863 which showed the agreement of the classified image with reference data [50, 51].

Finally, the raster image was converted into vector format, and each land unit on a pixel-by-pixel basis was assigned with the corresponding *C*-value suggested for each land use/land cover [40, 42]. It was further converted to a 30 m pixel size *C*-factor map using the C-value criteria for conversion (Table 3).

2.3.5. Management (Support) Practice (P-Factor). Land management factor is the ratio of soil loss from a particular management measure to the equivalent loss with up and down plowing [52]. It considers three methods, such as contours, cropping, and terraces that were important elements to control erosion [53]. However, in this study case, we identified that the majority of conservation measures have been constructed on farming lands, but the implementation lacks continuity (e.g., a plot treated with some conservation measures, but its neighbor is not), and there are limited conservation measures on nonagricultural lands. Therefore, the *P*-factor of the model was estimated through

Table 3: Literature recommended cover factor values of the study watershed.

Land use land cover	*C*-factor	Sources
Forest	0.01	Hurni [42]
Grazing land	0.05	Hurni [42]
Cultivated land	0.25	Hurni [42]
Shrub land	0.06	Wischmeier and Smith [40]

the alternative method that utilizes slope with land use/cover types recommended by the authors of [40] and effectively used by previous studies (e.g., [2, 54]; Table 4).

2.4. Soil Loss Relation with Some Site Physical Characteristics. The site-specific characteristics of the watershed mainly expressed in slope steepness, soil characteristics, and land cover and management determine the quantity of soil loss in the watershed. For instance, a model-based study reported by Belayneh et al. [2] found a high association between slope gradient and land use/cover in the Gumara watershed. The dominance of steep slope and undulating surface in a watershed increase the erosivity of runoff through the increased velocity of runoff water [12]. As the velocity of water increases, its shear stress on the surface and transportation sediment is higher [40]. The topographic characteristics are the main determinants for estimating soil loss, which measures the sediment transport capacity of the flow [46].

The natural cover of the land minimizes the raindrop impact and further decreases the volume of runoff by increasing on-site water infiltration. Conversely, barren and cultivated lands are exposed to be detached by raindrops and easily transported by running water. As a result, land use/cover characteristics of a watershed influence the rate of soil loss. Similarly, the soil characteristics of the site determine the rate of soil erosion. The dominancy of clay soils over sand and silts can cause high runoff and sediment loss [55]. The detachment and transport of soil particulates are especially higher at the beginning of the rainy season [55]. Heavy clay soil is distinguished as having lower infiltration capacities, and its infiltration capacity strongly decreases with increasing rainfall intensity and duration [56].

Therefore, the effect of site physical characteristics of the watershed was identified and quantified from the estimated soil loss map of the watershed using the zonal statistics toolset of ArcGIS. The physical characteristics of the watershed such as land use/cover map, slope category map, and soil type map were used as a zone to extract and quantify the mean soil loss, total soil loss, and area coverage. Finally, the variation was presented in average soil loss from each zone (t ha^{-1} $year^{-1}$).

3. Results and Discussion

3.1. RUSLE Parameters

3.1.1. Rainfall Erosivity (R) Factor. Twenty-two-year (2000–2022) mean maximum and minimum rainfall data of the area were 894.53 mm and 817.702 mm, respectively (Figure 3). The rainfall erosivity value of the watershed computed using [42] empirical equation revealed a minimum value of 1063 MJ mm ha^{-1} h^{-1} $year^{-1}$ and a maximum value of 1162.9 MJ mm ha^{-1} h^{-1} $year^{-1}$ of the area (Figure 3). The erosivity of rainfall in the watershed is high as compared to other areas in Ethiopia. This is mainly related to the fact that the annual rainfall in the area is very high appearing nearly nine months of the year in southwestern Ethiopia. As a result, it is commonly referred to as the wettest highland in Ethiopia. The relative spatial variability of rainfall erosivity in the watershed is higher in the western section than in all other sections. On the contrary, lower rainfall erosivity was observed in the eastern section of the watershed. The northern and southern portions of the watershed experienced similar erosivity with a slightly higher value in the northern section.

Table 4: Land management practice factor values considered in the watershed.

Land use land cover	Slope (%)	*P*-factor	Sources
Cultivated land	0–5	0.1	Wischmeier and Smith [40]
	5–10	0.12	
	10–20	0.14	
	20–30	0.19	
	30–50	0.25	
	50–100	0.33	
Others	All	1	

3.1.2. Slope Length and Slope Steepness (LS) Factor. The topographic factor values (*LS*-value) of the watershed ranged from 0.8 in low flow concentration level slope land to 55.4 in very steep slope areas (Figure 4). High slope steepness and length values dominate the watershed, and this is due to the fact that the area is situated dominantly within rugged terrain, in which 47% of the watershed area has a slope gradient of greater than 15%. A similar range of values was stated from Northwest Ethiopia [2, 25]. In this regard, the middle portion of the watershed experienced a higher LS value.

3.1.3. Soil Erodibility (K–Factor). The Majang watershed is covered by reddish Acrisols in the upper part of the watershed, brownish Cambisols in the middle part of the watershed, and black Nitisols in the lower part of the watershed. Soil erodibility is expressed as the vulnerability of the soil to be dispersed and transported by rainfall. In this regard, the erodibility value of soil in the area ranges from 0.02 to 0.9, in which a higher value indicates more susceptibility while a lower value indicates less susceptibility to erosion (Figure 5). Besides, the study watershed is dominated by red-colored soil, which contributes to high soil erosion in the area.

3.1.4. Land Use Land Cover (C–Factor). The Majang watershed was classified into four land use classes generated from Landsat 8-OLI -2021 by applying the maximum likelihood of supervised classification. The C-factor values range from 0.01 to 0.25 (Figure 6).

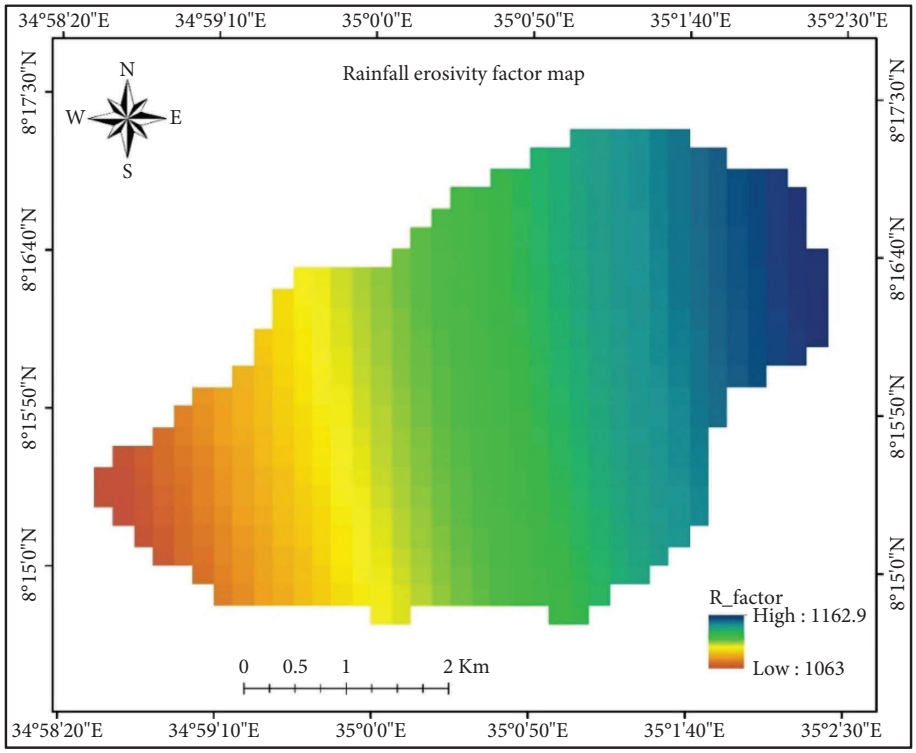

Figure 3: Map of rainfall erosivity factor (*R*-value) of Majang watershed.

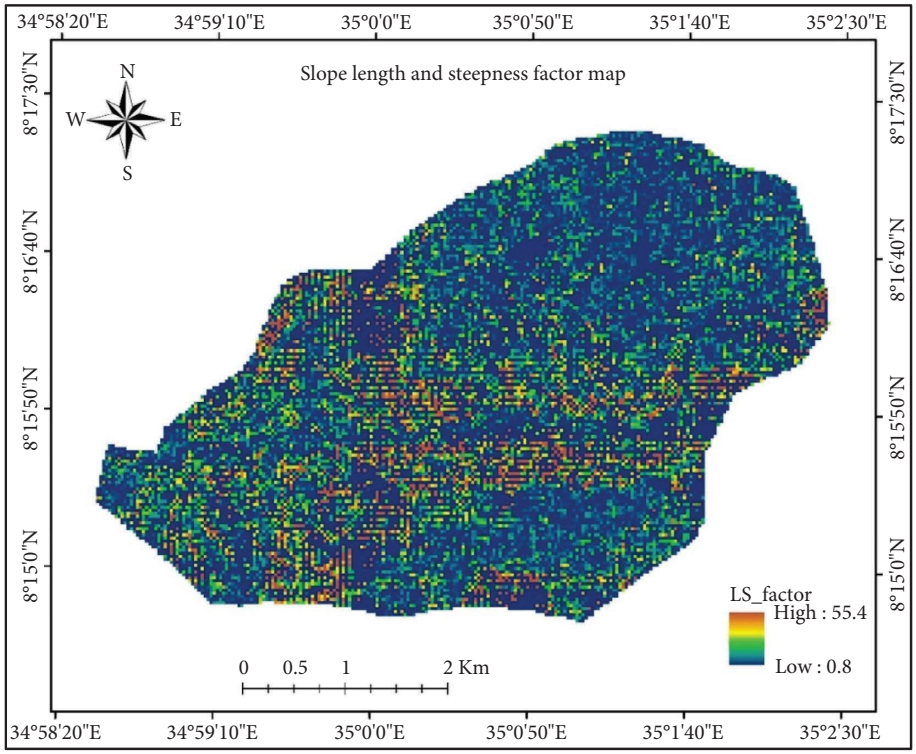

Figure 4: Slope length and steepness factor (LS) map of Majang watershed.

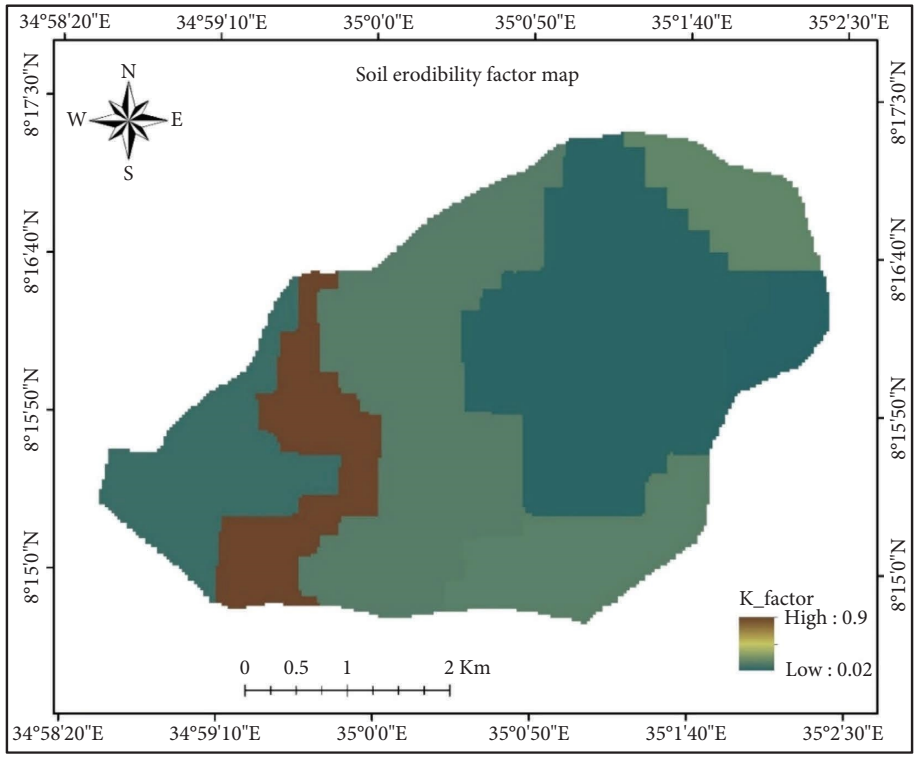

Figure 5: Erodibility value (*K*-factor) of Majang watershed map.

3.1.5. Soil Erosion Management Practice Factor (P Value). *P*-factor indicates the rate of soil loss according to agricultural practice and the influences of erosion by modifying the runoff flow characteristics [52]. The management practice factor value is between 0.1 and 1 in this study (Figure 7). In line with this, the survey results indicated that inappropriate use of agricultural land was among the main causes of the occurrences of soil erosion in the area. This is due to the fact that the farmers in the area cultivate different annual crops without appropriate land management practices. This actually leads to and attributes to the occurrences of high loss of soil and runoff in the area.

3.2. Estimated Soil Loss from the Majang Watershed. Currently, the Majang watershed was estimated to lose on average 30.6 t ha^{-1} year^{-1} (around a total of 74, 000 tons of soil annually) (Table 5; Figure 8). The potential annual soil loss of the watershed ranged from 0.04 in gentle-slope areas to 171.99 t ha^{-1} year^{-1} in the steepest part of the watershed. The estimated average soil loss result is smaller in our study watershed compared to other watersheds mainly in the northern and northwestern and central parts of the country. This might be due to a better forest cover of the area and a relatively gentler landscape.

Nevertheless, the current results of the study are greater than the tolerable level of soil loss studied for the highlands of Ethiopia (2–18 t ha^{-1} year^{-1} across different elevation and rainfall regimes) [42]. The current estimate (30.6 t ha^{-1} year^{-1}) nearly agrees with the findings stated in various regions of the country [22, 25, 57–59]. However, it showed a lower rate of erosion than some previous studies in different parts of the country mainly in the northwestern highlands [2, 23, 54, 60–62]. This discrepancy may occur due to the fact that the northwestern part of Ethiopian highlands is characterized by relatively high and torrential rainfall [2], and the land is intensively and continuously cultivated for millennia. However, in the southwestern highlands (of which the Majang watershed is a part), intensive cultivation and forest land cultivation is a recent phenomenon. Although the rainfall and its erosivity is comparable, the Majang watershed is characterized by better soil cover and less manipulated soil than the northwestern highlands.

The statistics result from the modeled soil loss map revealed greater dynamics of soil loss over space in the watershed. In this regard, the standard deviation value 48.43 t ha^{-1} year^{-1} showed the presence of high variability of soil loss. The variability is highly related to the variation in the RUSLE input parameters at different sites in the watershed [2]. For instance, sites with steep-slope cultivated topographies generate a high quantity of soil loss than gentle-slope forest areas.

3.3. The Effect of Site Characteristics on the Rate of Soil Loss Majang Watershed

3.3.1. Soil Losses in Various Land Use/Land Covers. The estimated average soil erosion rates under different land use/land cover types varied from 12 to 35^{-1} t ha^{-1} year^{-1}. In this regard, cultivated land is the most vulnerable type of land use (35.1 t ha^{-1} year^{-1}) followed by grasslands (19.6 t ha^{-1} year^{-1}) in the watershed (Table 6). The vulnerability of cultivated land to erosion could be attributed to cultivation

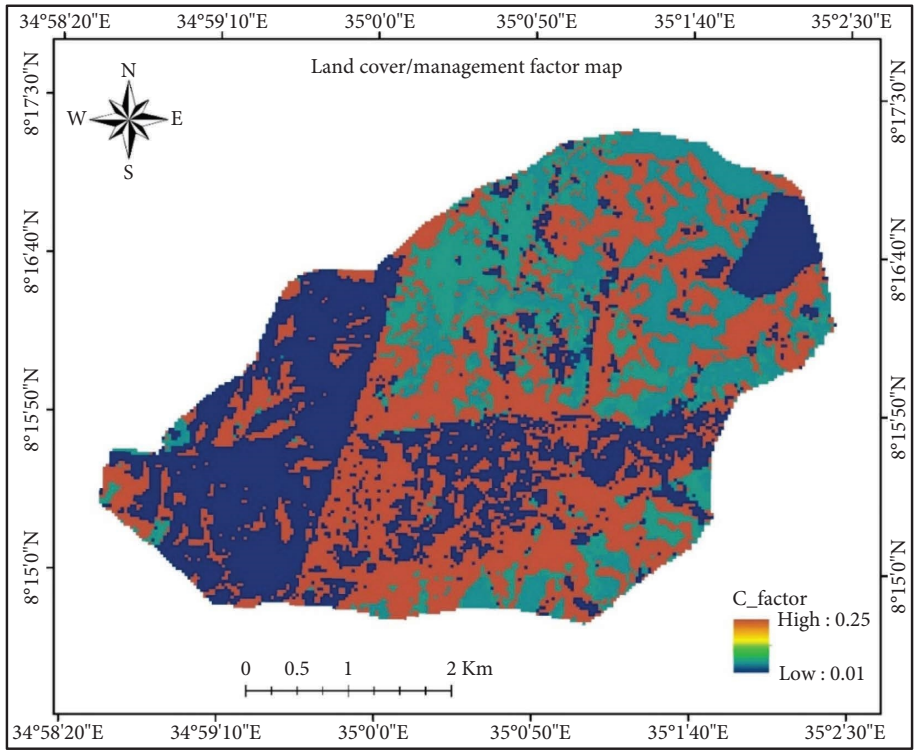

Figure 6: Land use land cover (*C*-factor).

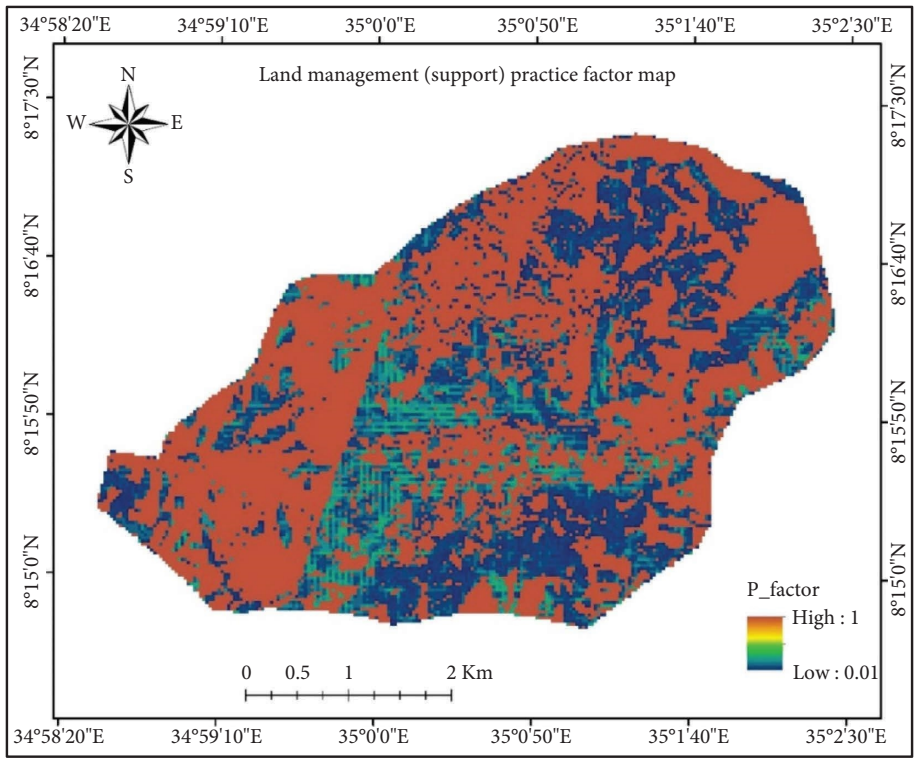

Figure 7: Erosion management practice factor (*P* value) Majang watershed.

and poor management practices. Conversely, forest land is found to be the least vulnerable land use and generated a very low amount of soil loss in total and rate of soil loss (12 t ha^{-1} $year^{-1}$).

Our estimates were in agreement with the findings of [2, 61] who reported that cultivated land was found to be the most vulnerable, which is a pillar of livelihood for about 84% of the population in Ethiopia. It implies that the agricultural

Table 5: Descriptive statistics of estimated soil loss in the Majang watershed.

Watershed	Area (ha)	Soil loss value in t ha^{-1} year^{-1}					Total (t year^{-1})
		Min	Max	Range	Mean	STD	
Majang watershed	2169.2	0.04	171.99	171.9	30.6	48.43	73839.428

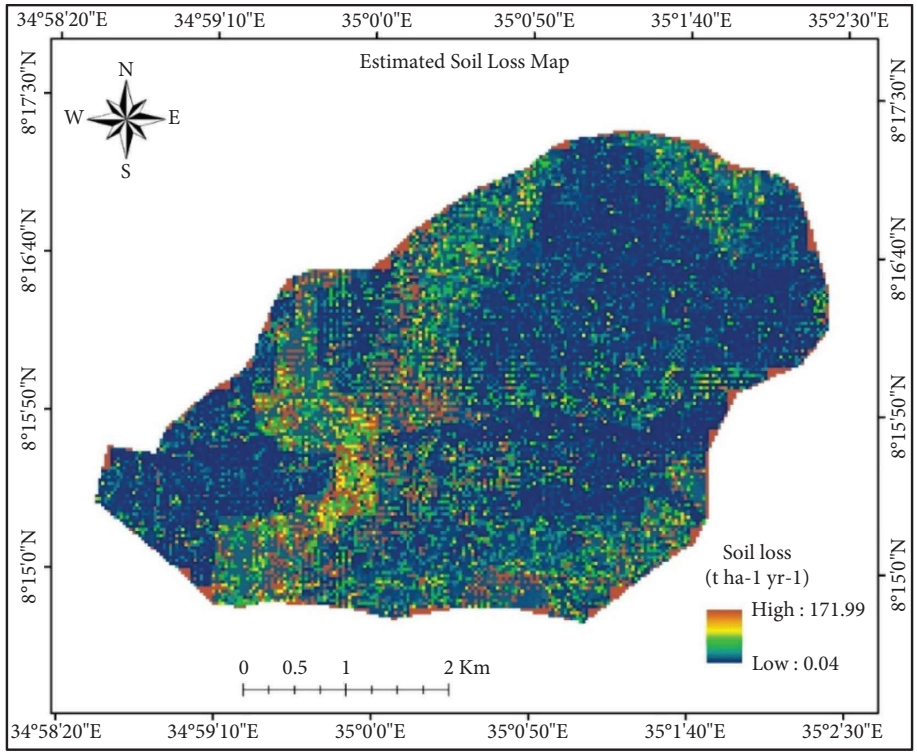

Figure 8: Soil erosion (soil loss) map of the Majang watershed.

production and productivity of the land and food security are threatened by soil erosion. This is because the average soil loss from the cultivated land (35.1 t ha^{-1} year^{-1}) is much greater than the rate of soil loss tolerance, which gradually leads to soil degradation and reduction of productivity. This might further call for supporting sustainable soil and water conservation measures for the safety of the ecosystem [63]. Soil and water conservation measures play an important role in both soil and water conservation. Soil and water conservation increases surface infiltration and reduces runoff amount, which further reduces soil degradation.

3.3.2. Soil Loss Variation under Different Slope Classes. According to the slope classification, the minimum amount of mean soil loss from the level to the gentler slope was found to be 7.8 t ha^{-1} year^{-1}, followed by 13.6 t ha^{-1} year^{-1} and 21.8 t ha^{-1} year^{-1} under 5–10 (strongly sloping slope) and 10–15 (moderately steep), respectively. Similarly, very steep slope classes (>30%) generated 62.8 t ha^{-1} year^{-1} (Table 7). This shows the existence of a strong relationship between sheet and rill erosion and slope gradient. Meaning soil removal increases with an increase in slope. As the slope gradient increases particularly in the agricultural landscapes, the soil vulnerability to downward movement either by gravity or by running water becomes very high. The visual interpretation of the soil loss map of the watershed (Figure 9) indicates that pixels generating high soil loss are found in the undulating steep slopes. This result was consistent with the studies of [2, 31, 61] which revealed that soil erosion rates increase with an increase in slope gradient. A similar study by [45] stated that the spatial distributions of the high spot area for soil erosion in the Anjeni watershed were found along the steeper slope of the Minchit and Zikire twin microwatersheds.

Table 6: Area coverage and rate of soil loss modeled for different land use land covers in the Majang watershed.

Class name	Area (ha)	Mean soil loss (t ha^{-1} year^{-1})
Forest land	729.4	12
Woodland	622.4	18.5
Shrub land	266.3	16.9
Cultivated land	258.8	35.1
Grassland	293.1	19.4

3.3.3. Soil Loss Variation under Different Soil Types. The erodibility nature of the soil strongly determines soil loss in a watershed. Black-colored soils with higher organic matter

Table 7: Rate of soil erosion under different slope conditions.

Gradient (%)	Area (ha)	Soil loss (t ha^{-1} year^{-1})
<5 (level to gentle sloping)	250	7.8
5–10 (strongly sloping)	1041.4	13.6
10–15 (moderately steep slope)	561.8	21.8
15–30 (steep slope)	183.4	37.7
>30 (very steep slope)	115.1	62.8

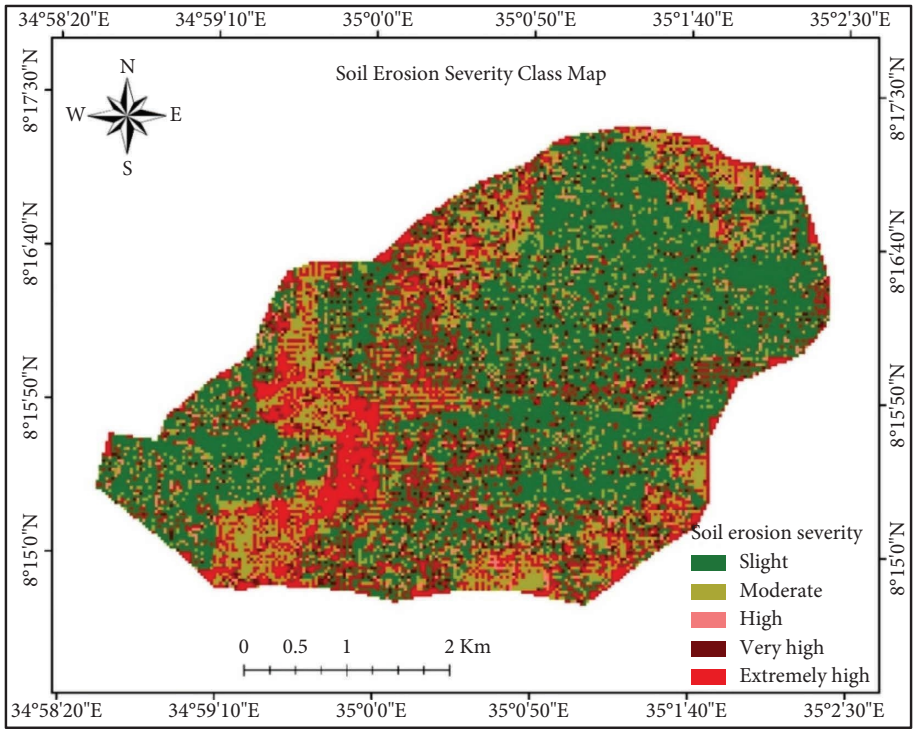

Figure 9: Soil erosion risk class map of Majang watershed.

content relatively resist erosion and soil loss than that of reddish, yellowish, or other types of colors with less organic matter content [40, 42]. Heavy clay soils mostly cause high runoff and sediment loss mainly at the beginning of the rainy season, which makes the soil easily detached and transported [55]. Because by nature, heavy clay soil is characterized by low infiltration capacity when the rainfall is highly intensive and stays for a longer duration [56]. Besides, the structure of the soil affects the amount of runoff and sediment detachment. In this study, the soil loss rate was highest under nonfertile Acrisols (28 t ha^{-1} yr^{-1}) and lowest in Dystric Cambisols (15.8 t ha^{-1} year^{-1}) (Table 8). Although the Acrisols covered a relatively gentler slope section of the watershed, due to their reddish and lower organic matter content, they lost a higher amount of average soil loss. On the contrary, lower average soil loss was estimated from the areas covered by brownish Cambisols and black Nitisols. In this regard, in the watershed, the erosion-resistant soil type (Dystric Cambisols) is dominant in plain areas, which are relatively less susceptible to soil erosion and generated only 15.8 t ha^{-1} year^{-1}. This indicates that the flatness of the slope and the presence of erosion-resistant soil types played a significant role to limit the soil loss rate in the lower topography of the area. On the other hand, a relatively greater amount of annual soil loss (28 t ha^{-1} year^{-1}) was generated from nonfertile Acrisols, from the upper topography of the watershed, which requires immediate important management practices (Table 9).

Table 8: Effects of soil type on rate of soil loss in the Majang watershed.

Soil types	Area (ha)	Mean soil loss (t ha^{-1} year^{-1})
Dystric Nitisols	276	19.5
Orthic Acrisols	631	28
Dystric Cambisols	1285	15.8

3.4. Vulnerable Areas (Erosion Hotspots) for Conservation Priority in Majang Watershed. As we have presented in Section 3.3, site characteristics predominantly affect the vulnerability of the plot (pixel) to soil erosion. Identifying the management areas based on the severity of soil erosion is

Table 9: Area coverage and proportion of soil erosion risk classes.

Erosion class (t ha^{-1} year^{-1})		Soil loss value in t ha^{-1} year^{-1}					Total (t year^{-1})	Area	
		Min	Max	Range	Mean	STD		ha	%
Slight	>11	0.0	11.0	11.0	3.7	3.0	4612.63	1128.69	52.0
Moderate	11–18	11.0	18.0	7.0	14.3	1.7	6191.55	390.69	18.0
High	18–30	18.0	30.0	12.0	23.6	3.5	3197.3	122.04	5.6
Very high	30–50	30.0	50.0	20.0	39.3	5.8	4859.74	111.42	5.1
Extremely high	>50	50.0	172.0	122.0	118.8	46.4	54978.21	416.52	19.2

very important for planning and implementing appropriate and priority-based development of conservation initiatives. Based on the soil erosion severity map, the area was classified into five soil loss severity classes such as slight (52%), moderate (18%), high (5.6%), very high (5.1%), and extremely high (19.2%) risk classes, and their estimated mean annual soil losses were ranged from slight risk classes (3.7 t ha^{-1} year^{-1}) to extremely high-risk classes (118.8 t ha^{-1} year^{-1}) (Table 8; Figure 9), which is significantly larger than the tolerable zone of highland Ethiopia (2–18 t ha^{-1} year^{-1}). Of the total area of the Majang watershed, 30% experienced high to extremely high soil erosion risk (Table 9). Similarly, the largest amount of soil loss was generated from extremely high (19.2%) risk class despite having a small area (19.2%) (with a minimum of 50 and a maximum of 172 t ha^{-1} year^{-1}).

This indicates that a substantial amount of soil losses was generated from the small areas of high, very high, and extremely high-risk classes (Table 9; Figure 9). It was due to the slope steepness of the area, lack of sustainable support practice (high *P*-factor value), and soil types which are less resistant to soil runoff of the area that facilitated the largest amount of soil losses from smaller areas of the watershed. The result was in agreement with the findings of [22, 57, 64, 65], who reported in their studies that the small proportion of the area of the watershed contributed to a significant amount of soil losses.

4. Conclusion

Soil erosion is one of the most damaging environmental problems and has contributed significantly to the loss of soil in the highlands of Ethiopia. Identification of severity classes and spatial distribution of the quantity of soil losses, soil erosion rate, and its relation with site physical characteristics using the GIS-based RUSLE model is important for the effective implementation of conservation measures and the planning process. The study finding revealed that soil erosion in the Majang watershed, in general, is high and considered to be a threat to agriculture because the soil loss from the agricultural land is higher (35.1 t ha^{-1} year^{-1}) as compared to the mean soil loss and soil loss tolerance (2–18 t ha^{-1} year^{-1}). The potential soil loss of the watershed is 30.6 t ha^{-1} year^{-1} (with a range between 0.04 and 171.99 t ha^{-1} year^{-1}). The study further implies that the majority of the soil loss was generated from the steep slope undulating topography, cultivated land, and nonfertile Acrisols. The slope steepness of the area coupled with continuous cultivation, lack of sustainable support practice, and soil types of the area contributed to the high amount of soil losses from smaller areas of the watershed. Hence, sustainable community-based conservation programs should be undertaken mainly in the identified erosion hotspot areas by involving all farmers/stakeholders. Furthermore, recurrent training programs need to be arranged for the local community on the effect of soil erosion and conservation issues.

Data Availability

The datasets used and/or analyzed during the current study are available from the corresponding author upon reasonable request.

Conflicts of Interest

The authors declare that they have no conflicts of interest.

Acknowledgments

The authors would like to thank data collectors and the community in the watershed for their assistance during data collection. This research was financially supported by Mettu University.

References

[1] G. W. Haile and M. Fetene, "Assessment of soil erosion hazard in Kilie catchment, East Shoa, Ethiopia," *Land Degradation & Development*, vol. 23, no. 3, pp. 293–306, 2012.

[2] M. Belayneh, T. Yirgu, and D. Tsegaye, "Potential soil erosion estimation and area prioritization for better conservation planning in Gumara watershed using RUSLE and GIS techniques," *Environmental Systems Research*, vol. 8, p. 20, 2019.

[3] C. Jiang, L. Zhao, J. Dai et al., "Examining the soil erosion responses to ecological restoration programs and landscape drivers: a spatial econometric perspective," *Journal of Arid Environments*, vol. 183, Article ID 104255, 2020.

[4] J. Poesen, "Soil erosion in the anthropocene: research needs: soil erosion in the anthropocene," *Earth Surface Processes and Landforms*, vol. 43, no. 1, pp. 64–84, 2018.

[5] P. Borrelli, D. A. Robinson, P. Panagos et al., "Land use and climate change impacts on global soil erosion by water (2015–2070)," *Proceedings of the National Academy of Sciences*, vol. 117, no. 36, pp. 21994–22001, 2020.

[6] R. Menendez-Duarte, J. Marquez, S. Fern_andez-Men_endez, and R. Santos, "Incised channels and gully erosion in Northern Iberian Peninsula: controls and geomorphic setting," *Catena*, vol. 71, no. 2, 2007.

[7] D. Wuepper, P. Borrelli, and R. Finger, "Countries and the global rate of soil erosion," *Nature Sustainability*, vol. 3, no. 1, pp. 51–55, 2019.

[8] M. Yibeltal, A. Tsunekawa, N. Haregeweyn et al., "Analysis of long-term gully dynamics in different agro-ecology settings," *Catena*, vol. 179, pp. 160–174, 2019.

[9] L. R. Oldeman, *Global extent of soil degradation*, Bi-annual report 1991–1992/ISRIC. ISRIC, Wageningen, The Netherlands, 1992.

[10] R. Lal, "Soil degradation by erosion," *Land Degradation & Development*, vol. 12, no. 6, pp. 519–539, 2001.

[11] M. Belayneh, T. Yirgu, and D. Tsegaye, "Current extent, temporal trends, and rates of gully erosion in the Gumara watershed, Northwestern Ethiopia," *Global Ecology and Conservation*, vol. 24, pp. e01255–55, 2020.

[12] T. Molla and B. Sisheber, "Estimating soil erosion risk and evaluating erosion control measures for soil conservation planning at Koga watershed in the highlands of Ethiopia," *Solid Earth*, vol. 8, no. 1, pp. 13–25, 2017.

[13] T. K. Alexandridis, A. M. Sotiropoulou, G. Bilas, N. Karapetsas, and N. G. Silleos, "The effects of seasonality in estimating the C-factor of soil erosion studies," *Land Degradation & Development*, vol. 26, no. 6, pp. 596–603, 2015.

[14] D. M. Moges and H. G. Bhat, "Watershed degradation and management practices in north-western highland Ethiopia," *Environmental Monitoring and Assessment*, vol. 192, no. 10, pp. 1–15, 2020.

[15] G. Ayalew, "A geographic information system based soil loss and sediment estimation in zingin watershed for conservation planning, highlands of Ethiopia," *International Journal of Science, Technology and Society*, vol. 3, no. 1, pp. 28–35, 2015.

[16] E. Gürtekin and O. Gökçe, "Estimation of erosion risk of Harebakayiş sub-watershed, Elazig, Turkey, using GIS based RUSLE model," *Environmental Challenges*, vol. 5, pp. 100315–315, 2021.

[17] K. K. Bahadur, "Spatio-temporal patterns of agricultural expansion and its effect on watershed degradation: a case from the mountains of Nepal," *Environmental Earth Sciences*, vol. 65, pp. 20–63, 2012.

[18] G. W. Haile and M. Fetene, "Assessment of soil erosion hazard in kilie catchment, east, Ethiopia," *Land Degradation & Development*, vol. 23, pp. 93–306, 2012.

[19] B. P. Ganasri and H. Ramesh, "Assessment of soil erosion by RUSLE model using remote sensing and GIS-A case study of Nethravathi Basin," *Geoscience Frontiers*, vol. 7, no. 6, pp. 953–961, 2016.

[20] A. K. Taloor, V. Kumar, V. K. Singh et al., "Land use land cover dynamics using remote sensing and GIS techniques in western doon valley, uttarakhand, India," in *Geoecology of Landscape Dynamics*, pp. 37–51, Springer, Singapore, 2020.

[21] W. Kebede, H. Tadesse, E. Garedew, and F. Yimer, "Soil erosion risk assessment in the Chaleleka wetland watershed, Central Rift Valley of Ethiopia," *Environmental Systems Research*, vol. 4, pp. 1–12, 2015.

[22] T. Gashaw, T. Tulu, and M. Argaw, "Erosion risk assessment for prioritization of conservation measures in Geleda watershed, Blue Nile basin, Ethiopia," *Environmental Systems Research*, vol. 6, pp. 1–14, 2017.

[23] V. N. Balabathina, R. P. Raju, W. Mulualem, and G. Tadele, "Estimation of soil loss using remote sensing and GIS-based universal soil loss equation in northern catchment of Lake Tana Sub-basin, Upper Blue Nile Basin, Northwest Ethiopia," *Environmental Systems Research*, vol. 9, pp. 35–32, 2020.

[24] H. Hurni, M. Giger, H. Liniger et al., "Soils, agriculture and food security: the interplay between ecosystem functioning and human well-being," *Current Opinion in Environmental Sustainability*, vol. 15, pp. 25–34, 2015.

[25] N. Haregeweyn, A. Tsunekawa, J. Poesen et al., "Comprehensive assessment of soil erosion risk for better land use planning in river basins: case study of the Upper Blue Nile River," *Science of the Total Environment*, vol. 574, pp. 95–108, 2017.

[26] T. Fenta and O. Ali, "Challenges and prospects of Food security in Ethiopia," in *Proceedings of the Food Security Conference 2003*, pp. 13–15, PAJS, Addis Ababa, Ethiopia, Augest 2003.

[27] B. Shiferaw, J. Okello, and V. R. Reddy, "Challenges of adoption and adaptation of land and water management options in smallholder agriculture: synthesis of lessons and experiences," 2009, https://www.researchgate.net/publication/266064557_Challenges_of_Adoption_and_Adaptation_of_Land_and_Water_Management_Options_in_Smallholder_Agriculture_Synthesis_of_Lessons_and_Experiences.

[28] H. Hurni, S. Abate, A. Bantider et al., "Land degradation and sustainable land management in the highlands of Ethiopia," 2010, https://www.researchgate.net/publication/265645925_Land_degradation_and_sustainable_land_management_in_the_Highlands_of_Ethiopia.

[29] M. Fazzini, C. Bisci, and P. Billi, "The climate of Ethiopia," in *Landscapes and Landforms of Ethiopia*, Springer, Dordrecht, The Netherlands, 2015.

[30] A. Kertész, "The global problem of land degradation and desertification," *Hungarian Geographical Bulletin*, vol. 58, no. 1, pp. 19–31, 2009.

[31] W. Bewket and E. Teferi, "Assessment of soil erosion hazard and prioritization for treatment at the watershed level: case study in the Chemoga watershed, Blue Nile basin, Ethiopia," *Land Degradation & Development*, vol. 20, no. 6, pp. 609–622, 2009.

[32] G. Zeleke, "Landscape dynamics and soil erosion process modelling in the north-western Ethiopian highlands," 2000, https://www.researchgate.net/publication/33804549_Landscape_Dynamics_and_Soil_Erosion_Process_Modeling_in_the_North-Western_Ethiopian_Highlands.

[33] N. Haregeweyn, A. Tsunekawa, J. Nyssen et al., "Soil erosion and conservation in Ethiopia, "A review," *Progress in Physical Geography: Earth and Environment*, vol. 39, no. 6, pp. 750–774, 2015.

[34] M. Belayneh, "Factors affecting the adoption and effectiveness of soil and water conservation measures among small-holder rural farmers: the case of Gumara watershed," *Resources, Conservation & Recycling Advances*, vol. 18, Article ID 200159, 2023.

[35] T. Erkossa, A. Wudneh, B. Desalegn, and G. Taye, "Linking soil erosion to on-site financial cost: lessons from watersheds in the Blue Nile basin," *Solid Earth*, vol. 6, no. 2, pp. 765–774, 2015.

[36] D. Sultan, A. Tsunekawa, N. Haregeweyn et al., "Analyzing the runoff response to soil and water conservation measures in a tropical humid Ethiopian highland," *Physical Geography*, vol. 38, no. 5, pp. 423–447, 2017.

[37] M. Zerihun, M. S. Mohammedyasin, D. Sewnet, A. A. Adem, and M. Lakew, "Assessment of soil erosion using RUSLE, GIS and remote sensing in NW Ethiopia," *Geoderma Regional*, vol. 12, pp. 83–90, 2018.

[38] Bure Agricultural office, "Agricultural Annual report. Report on area and production of crops and impacts of erosion," pp. 10–14, 2022, https://cgspace.cgiar.org/bitstream/handle/10568/17270/ScreeningReport_Bure.pdf?sequence=1.

[39] M. Keblouti, L. Ouerdachi, and H. Boutaghane, "Spatial interpolation of annual precipitation in Annaba-Algeria-

comparison and evaluation of methods," *Energy Procedia*, vol. 18, pp. 468–475, 2012.

[40] W. H. Wischmeier and D. D. Smith, *Predicting Rainfall Erosion Losses: A Guide to Conservation Planning (No. 537)*, Department of Agriculture, Science and Education Administration, Imphal, Manipur, 1978.

[41] K. G. Renard, *Predicting Soil Erosion by Water: A Guide to Conservation Planning with the Revised Universal Soil Loss Equation (RUSLE)*, United States Government Printing, Washington, DC, USA, 1997.

[42] H. Hurni, "Erosion-productivity-conservation systems in Ethiopia," 1985, https://www.researchgate.net/profile/Hans-Hurni/publication/308052268_Erosion-productivity-conservation_systems_in_ethiopia/links/580e75db08ae51b863966f8b/Erosion-productivity-conservation-systems-in-ethiopia.pdf.

[43] V. Prasannakumar, H. Vijith, S. Abinod, and N. G. Geetha, "Estimation of soil erosion risk within a small mountainous sub-watershed in Kerala, India, using Revised Universal Soil Loss Equation (RUSLE) and geo-information technology," *Geoscience Frontiers*, vol. 3, no. 2, pp. 209–215, 2012.

[44] U. Helldén, "An assessment of woody biomass, community forests, land use and soil erosion in Ethiopia," *A Feasibility Study on the Use of Remote Sensing and GIS [geographical Information System]-Analysis for Planning Purposes in Developing Countries*, Lund University Press, Lund, Sweden, 1987.

[45] W. G. Alemu and A. M. Melesse, "Impacts of long-term conservation measures on ecosystem services in Northwest Ethiopia," *International Soil and Water Conservation Research*, vol. 8, no. 1, pp. 47–55, 2020.

[46] I. D. Moore and J. P. Wilson, "Length-slope factors for the revised universal soil loss equation: simplified method of estimation," *Journal of Soil and Water Conservation*, vol. 47, pp. 423–428, 1992.

[47] P. S. Robert and D. Hilborn, "Fact sheet: universal soil loss equation (USLE)," 2000, https://www.ontario.ca/page/universal-soil-loss-equation.

[48] I. D. Moore and G. J. Burch, "Physical basis of the length-slope factor in the universal soil loss equation," *Soil Science Society of America Journal*, vol. 50, no. 5, pp. 1294–1298, 1986.

[49] D. P. Van der Knijff, R. J. Jones, and L. Montanarella, "Soil erosion risk: assessment in Europe," 2000, https://www.unisdr.org/files/1581_ereurnew2.pdf.

[50] J. R. Landis and G. G. Koch, "The measurement of observer agreement for categorical data," *Biometrics*, vol. 33, no. 1, p. 159, 1977.

[51] R. G. Congalton and K. Green, *Assessing the Accuracy of Remotely Sensed Data: Principles and Practices*, CRC Press, Boca Raton, FL, USA, 2019.

[52] T. G. Pham, H. T. Nguyen, and M. Kappas, "Assessment of soil quality indicators under different agricultural land uses and topographic aspects in Central Vietnam," *International Soil and Water Conservation Research*, vol. 6, no. 4, pp. 280–288, 2018.

[53] C. S. Park, Y. S. Jung, J. H. Joo, and J. T. Lee, "Best management practices reducing soil loss in the saprolite piled upland in Hongcheon highland," *Korean Journal of Soil Science and Fertilizer*, vol. 38, pp. 119–126, 2005.

[54] H. S. Gelagay and A. S. Minale, "Soil loss estimation using GIS and remote sensing techniques: a case of Koga watershed, Northwestern Ethiopia," *International Soil and Water Conservation Research*, vol. 4, no. 2, pp. 126–136, 2016.

[55] M. Bashari, H. R. Moradi, M. M. Kheirkhah, and M. Jafari-Khaledi, "Temporal variations of runoff and sediment in different soil clay contents using simulated conditions," *Soil and Water Research*, vol. 8, no. 3, pp. 124–132, 2013.

[56] W. Critchley, K. Siegert, and C. Chapman, *Water harvesting: a manual for the design and construction of water harvesting schemes for plant production*, Food and Agriculture Organization of the United Nations, RomeAGL. MISC/17/91, Singapore, 1991.

[57] A. S. Minale, "Retrospective analysis of land cover and use dynamics in Gilgel Abbay Watershed by using GIS and remote sensing techniques, Northwestern Ethiopia," *International Journal of Geosciences*, vol. 4, no. 7, pp. 1003–1008, 2013.

[58] M. Masha, T. Yirgu, and M. Debele, "Impacts of land cover and greenness change on soil loss and erosion risk in damota area districts, southern Ethiopia," *Applied and Environmental Soil Science*, vol. 2021, Article ID 9148138, 14 pages, 2021.

[59] B. A. Miheretu and A. A. Yimer, "Estimating soil loss for sustainable land management planning at the Gelana sub-watershed, northern highlands of Ethiopia," *International Journal of River Basin Management*, vol. 16, no. 1, pp. 41–50, 2018.

[60] N. Kayet, K. Pathak, A. Chakrabarty, and S. Sahoo, "Evaluation of soil loss estimation using the RUSLE model and SCS-CN method in hillslope mining areas," *International Soil and Water Conservation Research*, vol. 6, no. 1, pp. 31–42, 2018.

[61] A. Ketema and G. S. Dwarakish, "Prioritization of sub-watersheds for conservation measures based on soil loss rate in Tibur Wuha watershed, Ethiopia," *Arabian Journal of Geosciences*, vol. 13, pp. 1–16, 2020.

[62] Y. Teshome, "Assessment of soil erosion hazard and contributing factors in the upper Domba Watershed," *Heliyon*, vol. 14, pp. 10–16, 2022.

[63] T. Amdemariam, "The effect of soil barriers stabilized with vetiver grass (vetiveria zizanioides) and tree lucerne (chamaecytisus palmensis) on selected soil properties and barley (hordeum spp.) yield: a case study from banja shikudad woreda, awi zone," *Tropical Land Resource Management*, Master's Degree Thesis, Mekele University, Mek'ele, Ethiopia, 2008.

[64] A. Shiferaw, "Estimating soil loss rates for soil conservation planning in the Borena Woreda of South Wollo Highlands, Ethiopia," *Journal of Sustainable Development in Africa*, vol. 13, pp. 87–106, 2011.

[65] V. J. Markose and K. S. Jayappa, "Soil loss estimation and prioritization of sub-watersheds of Kali River basin, Karnataka, India, using RUSLE and GIS," *Environmental Monitoring and Assessment*, vol. 188, no. 4, p. 225, 2016.